Planetary and Space Science 59 (2011) 1551–1558

Contents lists available at ScienceDirect

Planetary and Space Science

journal homepage: www.elsevier.com/locate/pss

Observations of dawn–dusk aligned polar cap aurora during the substorms of January 21, 2005

A.M. Du [a,*], W. Sun [b], B.T. Tsurutani [c], R.N. Boroyev [d], A.V. Moiseyev [d]

[a] Institute of Geology and Geophysics, Chinese Academy of Sciences, Beijing 100029, China
[b] Geophysical Institute, University of Alaska Fairbanks, AK 99775, USA
[c] Jet Propulsion Laboratory, California Institute of Technology, Pasadena, CA, USA
[d] Yu.G. Shafer Institute of Cosmophysical Research and Aeronomy, Yakutsk, Russia

ARTICLE INFO

Article history:
Received 26 February 2011
Received in revised form
11 June 2011
Accepted 14 June 2011
Available online 20 July 2011

Keywords:
Substorm
Planetary shock
Polar cap Aurora
Reconnection

ABSTRACT

A new type of polar cap aurora, dawn–dusk aligned polar cap aurora (DDAPCA), was detected during the exceptionally intense January 21, 2005 substorm (AE_{max}=3504 nT). The DDAPCA was located at very high latitude (> 85° MLAT) in the polar cap region. As the interplanetary magnetic field (IMF) GSM *By* component rotated from a positive to a negative value, the DDAPCA tilt angle relative to the dawn–dusk direction rotated anticlockwise and reached ~45°. It is speculated that the DDAPCA arises from the formation of an X-line in the distant (> 80R_E) tail due to polar cap magnetic field reconnection under unusually high solar wind compression conditions.

1. Introduction

By definition, most auroras occur within the auroral oval (65–70° MLAT in the midnight sector and 70–75° MLAT at noon). The oval becomes enlarged and is centered at lower latitudes with increasing levels of geomagnetic activity (Feldstein and Starkov, 1967). Auroras may also occur in the polar cap region during intervals of northward interplanetary magnetic fields (IMFs). Lassen and Danielsen (1989) studied Greenland discrete polar auroral arcs during 1963–1974 for fairly low magnetospheric disturbance levels (AE~41–50 nT). They found that arcs in the central polar cap are roughly aligned in the noon–midnight direction. These arcs were called "Sun-aligned arcs" or "θ-auroras". Polar cap auroras typically occur when the IMF *Bz* component is northward and thus the magnetosphere is quiet. With the onset of a substorm, the polar cap auroral arcs typically disappear.

Newell et al. (1999) analyzed the magnetic storm of January 10–11, 1997. The magnetic storm was caused by the southward IMF component of an interplanetary magnetic cloud. Newell et al. (1999) found that pairs of polar cap arcs became widely separated from the auroral oval, that is, an extremely rare double θ aurora configuration formed. This happened twice during the storm. The dynamics of these double θ-aurora events constrain any models of their origin.

Elphinstone et al. (1995) found that during the later stages of an auroral substorm, the luminosity distribution frequently resembles a double oval, one oval lying poleward of the normal or main UV auroral oval (< 72° MLAT). They interpreted the double oval morphology as being due to the plasma sheet boundary layer becoming active in the later stages of the substorm process. Kornilova and Kornilov (2006) proposed that the aurora activations at the polar and equatorward edges of double ovals are interrelated. This relationship was observed ~30–40 min before the breakup onset. Auroral arc activations may be initiated by weak visual and subvisual structures drifting poleward or equatorward in diffuse auroras and by luminosity inhomogeneities moving along the pre-breakup arc (Kornilova and Kornilov, 2006). Akasofu et al. (2010) mentioned that after the southward turning of the IMF, the equatorward half of the oval shifts rapidly equatorward, like a narrowing of the width of the equatorward half of the auroral oval. They believed that polarward arcs are quite independent of equatorward arcs.

The purpose of this paper is to present observations of a new type of polar cap arcs, DDAPCAs, which are considerably different from above-mentioned θ-auroras and double ovals. We focus on a particular case of an arc crossing the polar cap at very high MLAT, ~85–90°. The arc is aligned in the dawn-to-dusk direction. In conclusion, we will present a model for DDAPCA arc formation.

2. Observations

2.1. Solar wind and IMF observations

Fig. 1 shows the solar wind parameters and interplanetary magnetic field (observed by Cluster C1) and the geomagnetic

* Corresponding author.
E-mail address: amdu@mail.iggcas.ac.cn (A.M. Du).

0032-0633/$ - see front matter © 2011 Elsevier Ltd. All rights reserved.
doi:10.1016/j.pss.2011.06.021

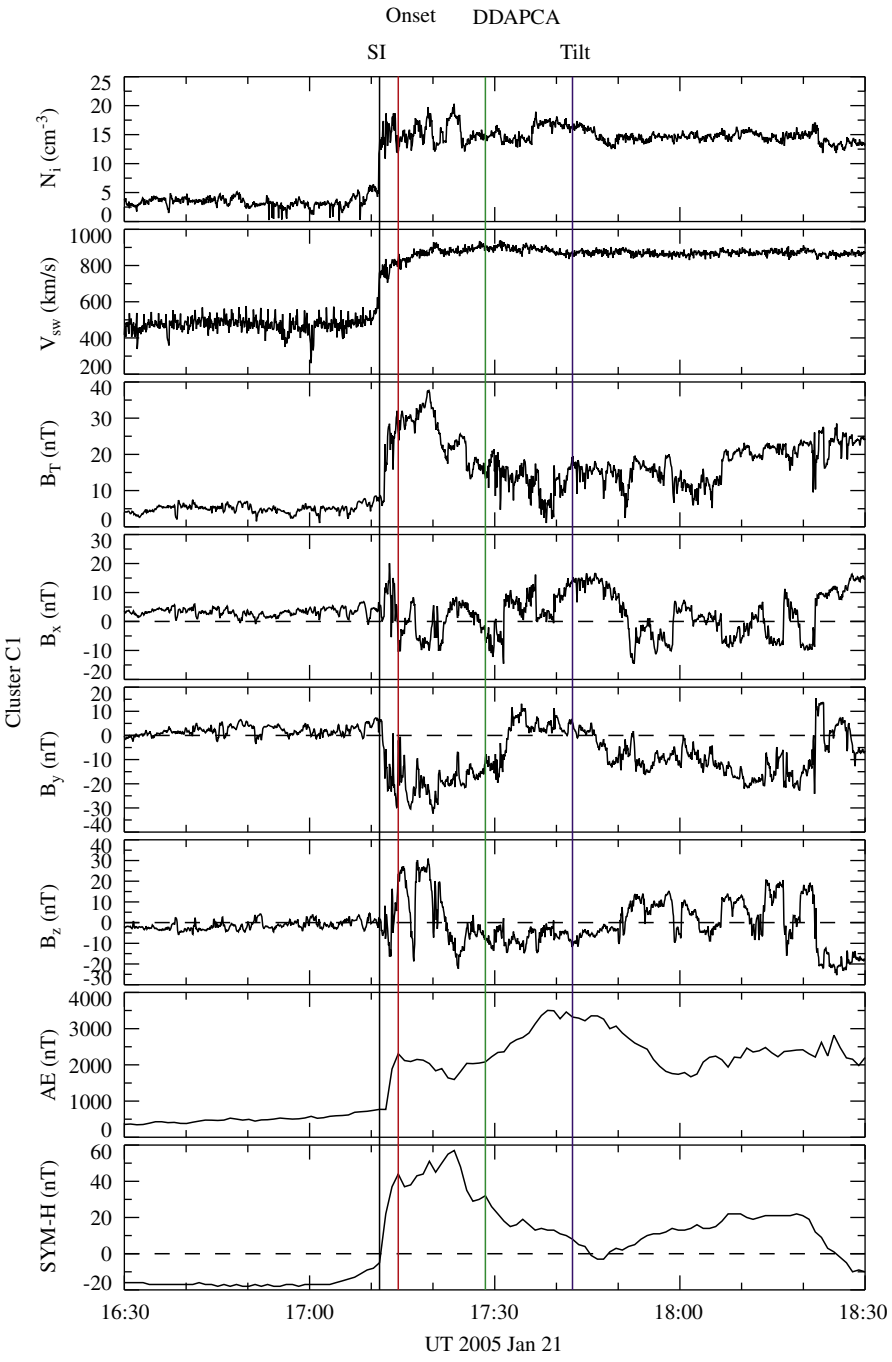

Fig. 1. Solar wind parameters and interplanetary magnetic field observed by Cluster C1, and the geomagnetic index AE and SYM-H during the interval of 1630–1830 UT on January 21, 2005. (For interpretation of the references to color in this figure, the reader is referred to the web version of this article.)

AE and SYM-H indices during 1630–1830 UT on January 21, 2005. Cluster C1 was located in the solar wind ($X\sim16R_E$ and $Y\sim10R_E$). An interplanetary shock was detected at ~1711 UT on January 21, 2005 (see Du et al., 2008). The shock is indicated by a vertical black line. The shock was found to be quasi-perpendicular with θ_{Bn} (the angle between the shock normal and the upstream magnetic field) determined to be 54°. A SI+ of +80 nT was created by the shock compression of the magnetosphere. The SI+ can be noted in the SYM-H index in Fig. 1. Following the shock, the AE index increased to ~2307 nT at 1714 UT indicating the expansive phase onset of the substorm. The IMF turned northward (vertical red line in Fig. 1), causing a short recovery for ~9 min with a decrease of the AE index to 1594 nT. As the IMF *Bz* turned southward again at 1737 UT, another substorm expansive phase occurred leading to a maximum AE of 3507 nT. Meanwhile, the SYM-H index decreased to ~0 nT, and no westward ring current developed. There was no occurrence of a geomagnetic storm main phase during this interal. At 1750 UT, the IMF *Bz* turned to northward once again. This was time-coincident with substorm recovery.

The geomagnetic storm on January 21, 2005 is a famous storm event due to the main phase developing during the northward IMF (Du et al., 2008). The solar and interplanetary conditions of this major storm were described in detail by Zhang et al. (2007)

and Echer et al. (2008). Echer et al. (2008) noted that shock strength is important for the amount of energy released into the magnetosphere/ionosphere.

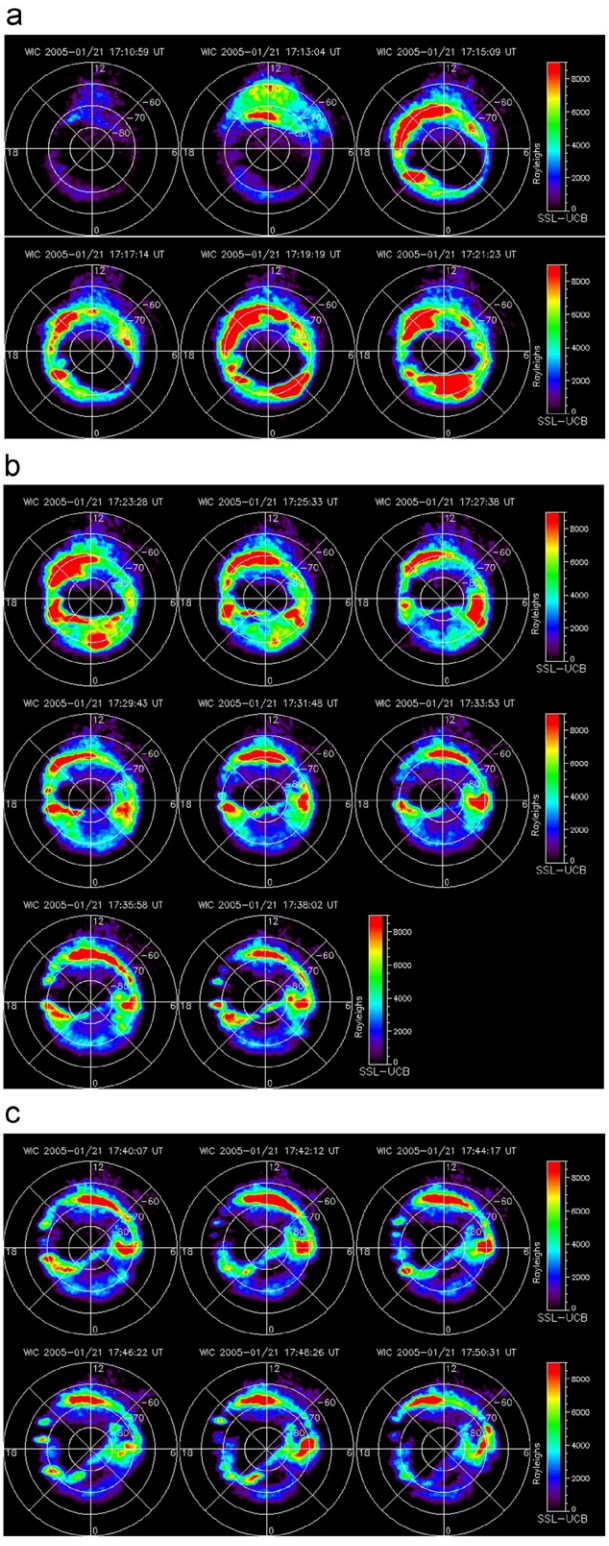

Fig. 2. (a) Wideband Imaging Camera (WIC) images taken by the IMAGE/FUV instrument from IMAGE satellite for dayside aurora, brightening and poleward expansion of nightside auroa during the interval of 1710–1721 UT on January 21, 2005; (b) The WIC images for evolution of the down–dusk arcs cross the polar cap during 1723–1738 UT; (c) The WIC images for anticlockwise rotation of the tilted DDAPCA during 1740–1750 UT.

2.2. Aurora observations

Polar auroral images taken by the IMAGE/FUV instrument (Mende et al., 2000a,b) are shown in Fig. 2a–c. The images proceed in time from the top left to the right and then down. Fig. 2a clearly shows that the dayside aurora was brightening around the noon at cusp latitudes of ~75° MLAT at 1711 UT (between the first and second images). The aurora expanded in all directions: poleward from 68° to 80° MLAT and longitudinally to morning (~07 MLT) and to afternoon (~15 MLT) by ~1713 UT. Afterwards, the dayside aurora extended mainly to the afternoon sector up to 18 MLT and joined with the developed nightside aurora. These auroral features have been called shock auroras (Tsurutani et al., 2001a) and the physical mechanism for their formation can be found in the above references.

Fig. 2a shows also that the nightside auroral oval was located at ~70° MLAT before the substorm expansion onset at 1713 UT. The nightside aurora first brightened in the midnight (~00 MLT) at ~70° MLAT at 1713 UT, indicating substorm expansion. After initial brightening, the aurora extended first towards the evening sector (21 MLT) and poleward to ~78° MLAT at 1715 UT. At 1719 UT, the auroral displaying reached to the morning sector (03 MLT). At ~1721 UT, the midnight sector aurora had its greatest luminosity and by then the aurora had expanded poleward to ~80° MLAT. It is noteworthy that there was no equatorward expansion.

Fig. 2b shows that the nightside aurora arc started to separate into two parts at the poleward and equatorward boundaries at ~1723 UT. The equatorward arc in the midnight sector became weak at ~1725 UT whereas the arcs at dawn and dusk intensified At ~1728 UT a part of the midnight sector aurora disappeared giving an aurora-less region from 76° to 84° MLT between 21 and 02 MLT. The overall configuration has been called a "horseshoe aurora" by Tsurutani et al. (1998) for the January 10–11, 1997 event, given the overall shape.

The remaining midnight sector auroral displays were a poleward boundary arc at 85° MLAT and an equatorward boundary arc at ~70° MLAT. This configuration of two arcs is quite different from the double oval proposed by Elphinstone et al. (1995) and

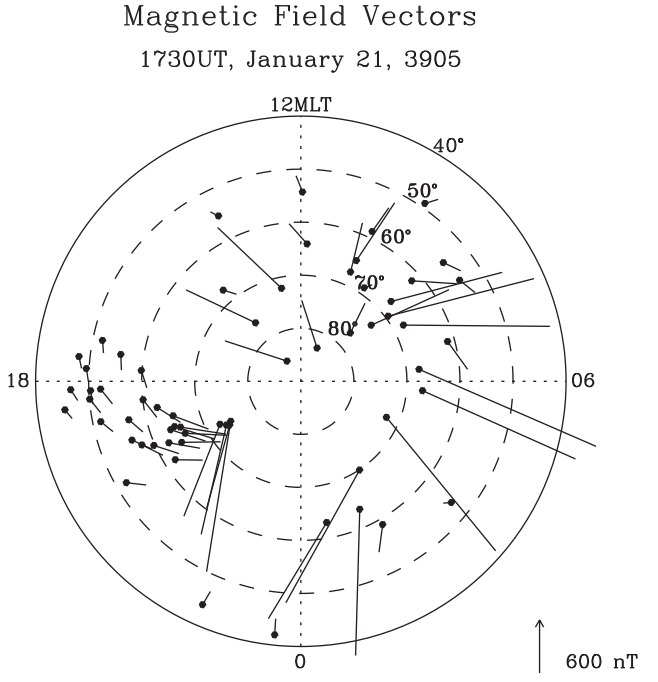

Fig. 3. Distribution of the horizontal components of the geomagnetic field perturbations observed at 62 observatories in polar region at ~1730 UT.

Kornilova and Kornilov (2006). In this case the poleward boundary arc is located at a very high latitude of ~85°. The poleward arc appears like a bridge cross the polar cap along dawn–dusk direction. After 1727 UT the equatorward boundary arc became less intense but remained at ~70° MLAT. As shown in Fig. 2c, at ~1742 UT the DDAPCA turned anticlockwise and reached a tilt angle of 45° with respect to the dawn–dusk direction. The arc also moved to ~90° MLAT. This auroral configuration was stable until ~1748 UT. The IMF *Bz* turned northward at ~1750 UT, and after that time, the DDAPCA intensity faded. The DDAPCA angle is correlated with the IMF *By* component switching from positive to negative values.

3. The ionospheric electrodynamic parameters

The KRM method is an algorithm scheme developed by Kamide et al. (1981). All ionospheric electrodynamic parameters including electric potential, horizontal current and field-aligned current can be inversed using the KRM method on the basis of ground-based magnetometer data.

In this case, sixty-two ground-based magnetometer observatory data with a time resolution of one minute were used as inputs to the KRM algorithm. The derived quantities are the electric potential, horizontal current vectors and field-aligned currents. Fig. 3 shows the distribution of the horizontal components of the geomagnetic field perturbations observed at 62 observatories at ~1730 UT covering the latitude range of ~50–90°.

Fig. 4 shows the ionospheric electric potential distribution at the same time as that in Fig. 2. Contours of the electric potential are spaced at 25 kV intervals. The potential extrema are indicated by a plus sign (solid line) and negative sign (dash line) for each cell. The maximum and minimum of the potential are shown in the lower left corner of each plot. Fig. 2 clearly identifies a positive potential cell in the center of the polar cap and a negative potential cell in the premidnight auroral region. It is worthy to note that the total electric potential is quite intense throughout the whole substorm interval. The total potential reached a maximum of ~600 kV coincident with the substorm peak intensity (at ~1740 UT).

At the substorm onset (~1713 UT) an intense southward electric field, E_s, can be found at 70° MLAT and 21 MLT in Fig. 4. E_s was intensified with time and was superimposed onto the original two-cell convection pattern. This type of feature has been previously noted during intense substorm expansion phases by

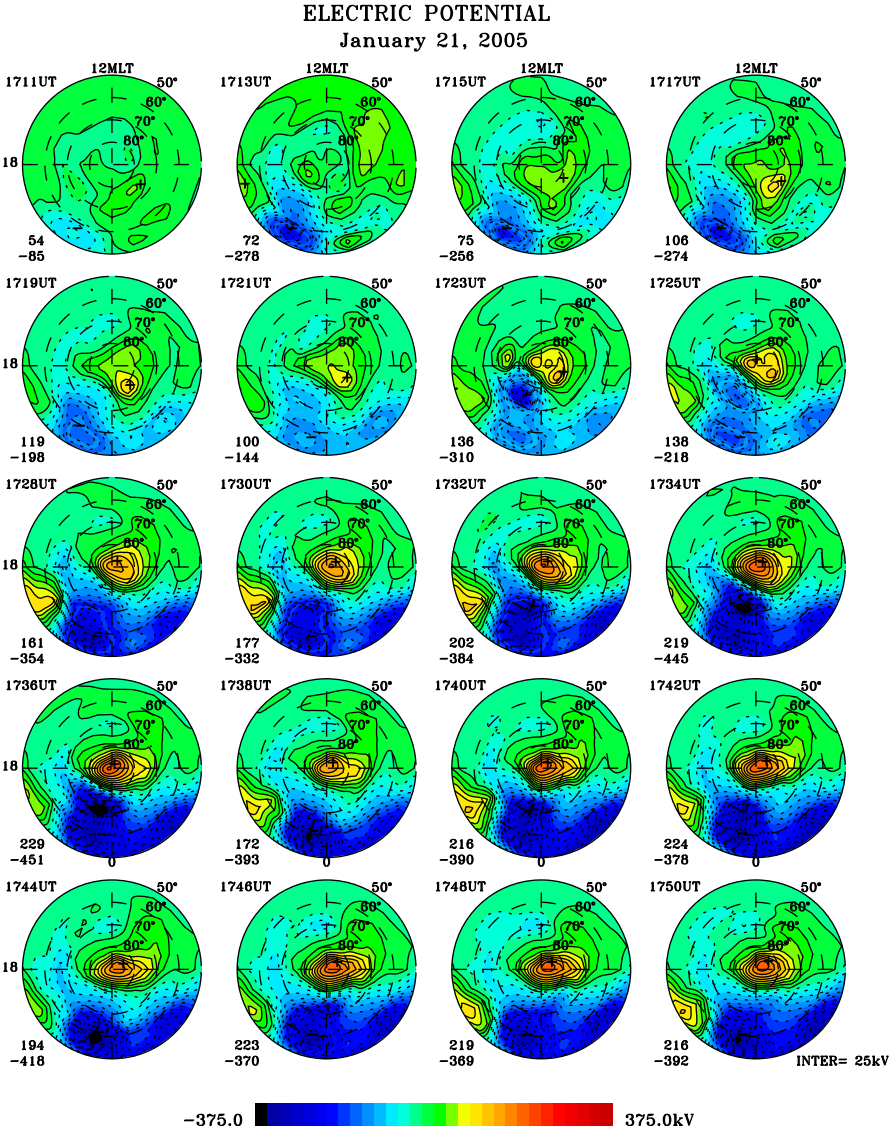

Fig. 4. Distribution of ionospheric electric potential obtained by the KRM algorithm at the same time as those in Fig. 2. (For interpretation of the references to color in this figure, the reader is referred to the web version of this article.)

Sun et al. (2008). However in the Sun et al. case, the formation of intense southward electric fields was related to intense westward nightside electrojets, unlike the case here. It rarely occurred that the boundary between the positive (red) and negative (blue) potential regions move poleward to $> \sim 80^\circ$ MLAT. In the present case this happened at 1723 UT.

For the electrical potential distribution as shown in Fig. 4, a continuous anticlockwise turning of 90° from a noon–midnight orientation (as for typical convection patterns) to a dawn–dusk direction at the maximum of substorm intensity (1740 UT) has been noted for the first time. During this interval from 1740 to 1750 UT, the IMF *Bz* became weak and negative (~ -10 nT) while the solar wind speed and ion density remained high. At $\sim$1740 UT, the IMF *By* turned from strongly negative to positive, and fluctuated around 5 nT.

Fig. 5 shows the derived ionospheric current vectors. The red vectors indicate westward currents and blue vectors eastward currents. Just after 1711 UT when the interplanetary shock impacted magnetopause, the substorm onset occurred at 1713 UT. The intense westward electrojet suddenly intensified from midnight at $\sim 65^\circ$ MLAT to afternoon at $\sim 70^\circ$ MLAT. Following the southward turning of the IMF at $\sim$1720 UT, a part of the electrojet in the morning sector moved to $\sim 70^\circ$ MLAT while the evening sector portion moved to $\sim 85^\circ$ MLAT. Afterward, the two currents gradually separated. The morning sector portion of the electrojet remained in place, while the evening part intensified and moved poleward. At $\sim$1740 UT when the substorm reached maximum intensity (AE$\sim$3600 nT), the evening sector portion of the electrojet turned to flow from dawn to dusk from $\sim 70^\circ$ to 90° MLAT. The most intense current was $\sim$10 A/m at the time of the peak of the first substorm.

Fig. 6 shows the distribution of field-aligned currents (FACs) obtained by the KRM algorithm. Very intense FACs developed during the substorm expansive phase. The intense FACs reached a peak value of $\sim 10.8\ \mu A/m^2$ at 1723 UT. It is interesting to note that intense upward FACs indicated by the deep blue color coincide well with dayside and equatorward nightside auroras (shown in Fig. 2). The dawn–dusk aligned polar cap aurora, which developed later, corresponds to downward FACs (indicated by the red color).

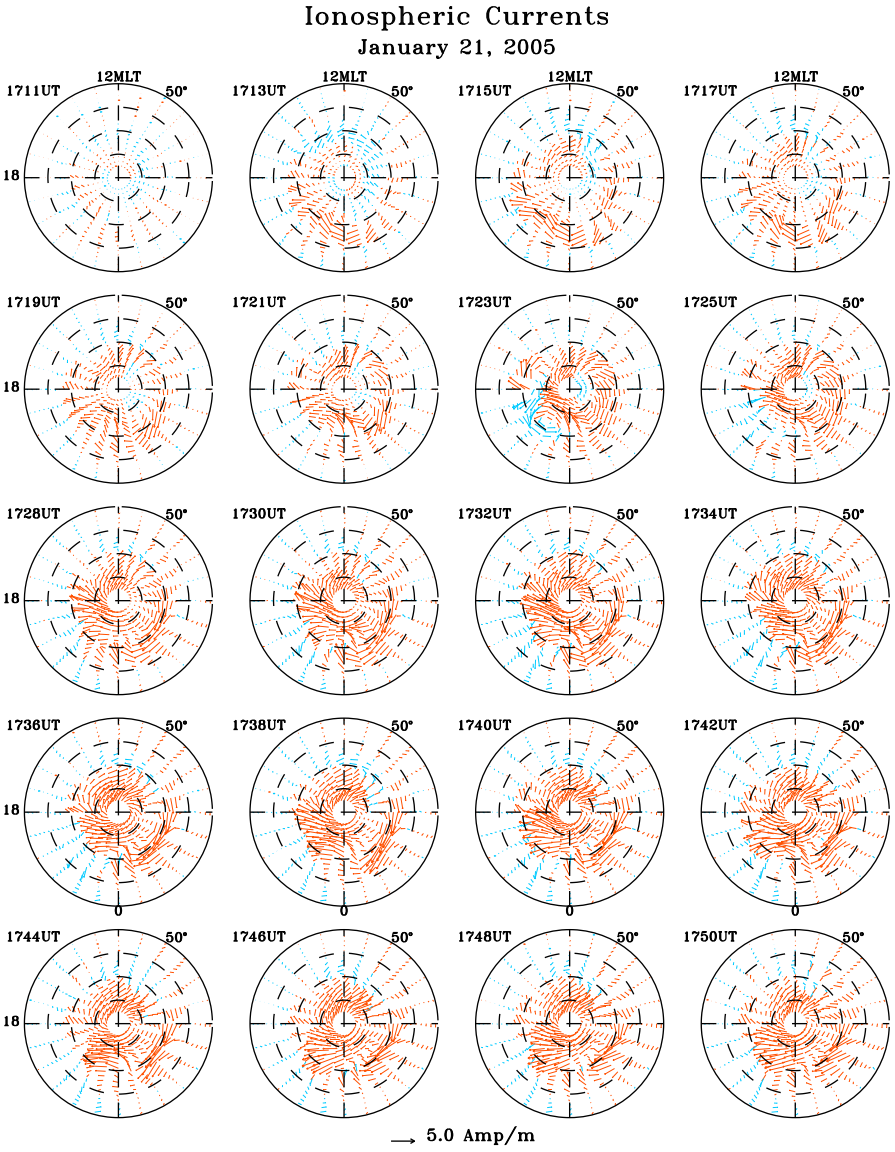

Fig. 5. Derived ionospheric current vectors obtained by the KRM algorithm. Red vectors indicate westward currents and blue vectors eastward currents. (For interpretation of the references to color in this figure legend, the reader is referred to the web version of this article.)

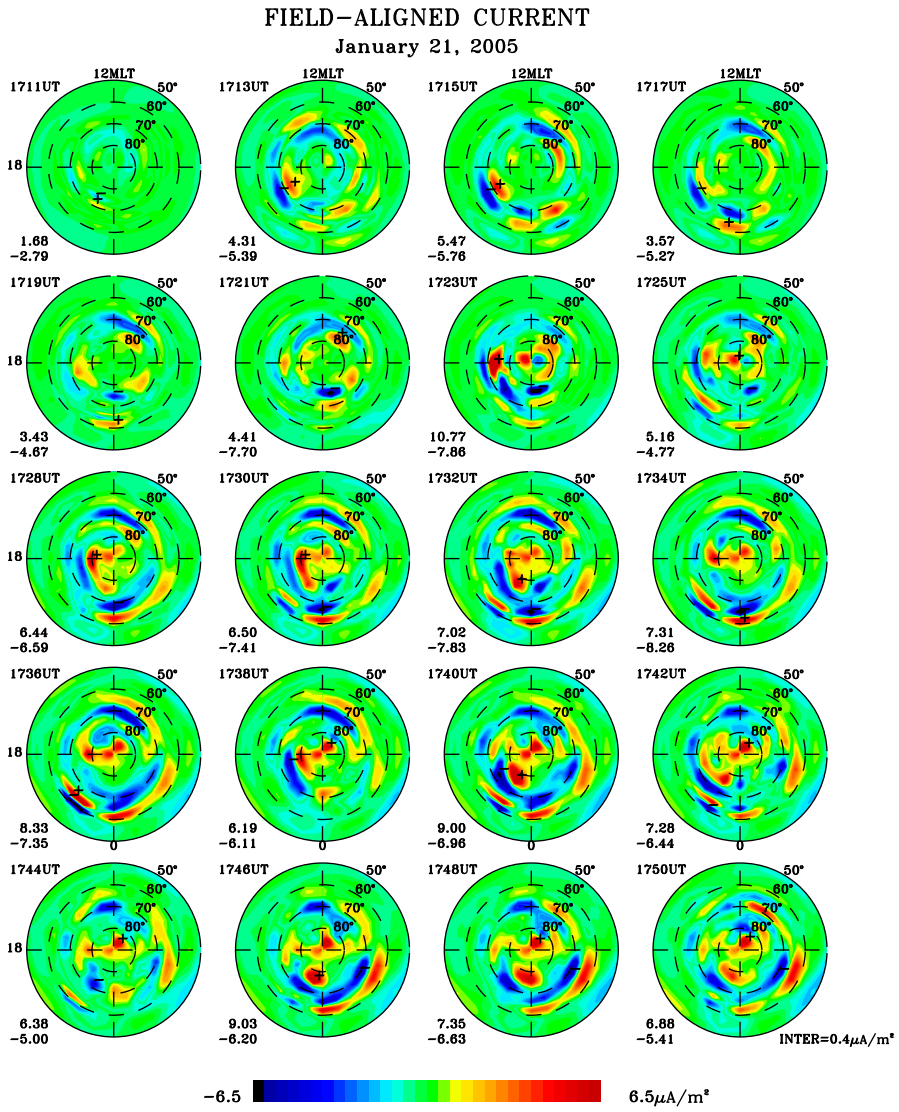

Fig. 6. Distribution of field-aligned currents (FAC) obtained by the KRM algorithm. The deep blue color indicates upward FACs, and red color the downward FACs. (For interpretation of the references to color in this figure legend, the reader is referred to the web version of this article.)

4. Discussion and summary

Summarizing the above observations, it can be noted that a dawn–dusk aligned polar cap aurora was detected when the IMF *Bz* was southward. The DDAPCA occurred during an intense substorm on January 21, 2005 and located at very high latitudes ($>85^\circ$ MLAT). As the IMF GSM *By* component rotated from positive to negative values, the DDAPCA angle rotated anticlockwise and reached a tilt angle of 45° relative to the dawn–dusk direction.

4.1. Dayside aurora triggered by an interplanetary shock

The impact of an interplanetary shock at ~1711 UT caused a normal substorm expansive phase onset at 1713 UT with a nightside aurora brightening at 70° MLAT. The AE index quickly increased to a maximum of 2307 nT. Then the auroral area expanded towards the evening, morning and poleward until 1723 UT and the AE index decreased to 1594 nT due to the IMF *Bz* turning northward. The intense substorm event occurred at 1713 UT might not have growth phase and was directly caused by an interplanetary shock.

The upward FACs as shown in Fig. 6 were enhanced in the cusp region of 70–80° MLAT at ~1713 UT. The precipitating electrons associated with the intense upward FACs excite active, discrete dayside aurora (Tsurutani et al., 2001b). Zhou et al. (2003) discussed that the possible mechanisms of field–aligned current generation are some dynamic processes occurring on the dayside magnetopause, such as magnetic shearing, magnetopause perturbation, magnetic reconnection and Alfvén wave generation. Echer et al. (2011) found that *AL* decreases usually occur within 10 min of shock impingement on the magnetopause, and the shock strength is important for the amount of energy released into the magnetosphere/ionosphere.

4.2. DDAPCA formation

The nightside aurora bulge started to be separated as the IMF *Bz* turned southward at 1723 UT. Such occurrences may produce a so-called double oval (Elphinstone et al., 1995). However the separated poleward arc moved quickly to very high latitude of 85–90° to form the DDAPCA. At the same time, the pattern of the ionospheric potential was highly distorted. Although the results of the KRM method can sometimes be affected by the distribution of ground-based observatories, Fig. 3 shows that for this event

there was good coverage of the horizontal components of the geomagnetic field perturbations. A surprising large north–south potential drop indicated a very strong southward electric field in the night side. It contributed to the formation of a westward electrojet and FACs. Finally a second substorm expansion occurred, characterized by the very high AE index of 3504 nT, a total electric potential of 680 kV, a westward electrojet of ~10 A/m and an upward FAC of 5.4 $\mu A/m^2$ in the polar cap. Such an intense substorm expansion at very high MLATs (in the polar cap) is not explained by current substorm models.

It is noted in Fig. 4 that the positive potential cell after 1723 UT was most likely part of the embedded lobe circulation Knipp (1993). At the nightside edge of the positive potential cell, the dawn–dusk aurora arc was formed. The most intense auroral precipitation was located on the dawn and dusk sides (flank auroras). For the flank aurora, one speculation is that particles pre-existing in the outer magnetosphere or transferred from the magnetosheath into the magnetosphere during the K–H instability (Otto and Fairfield, 2000; Nykyri and Otto, 2001) might be accelerated along the field-aligned currents and precipitated into the ionosphere. This scenario predicts the discrete auroras could occur in the ionosphere at the magnetic latitudes, which map to the LLBL (Zhou and Tsurutani, 2001; Zhou et al., 2001).

The dayside aurora in the IMAGE WIC data coincided with intense, high-latitude upward FACs (indicated by the deep blue color in Fig. 6). The DDAPCA, which developed later corresponds to downward FACs (indicated by the red color). The intense nightside upward FACs (indicated by the deep blue color) coincided well with equatorward nightside aurora.

4.3. Possible mechanism of the DDAPCA

The DDAPCA was located at extremely high latitudes of 85–90° where the magnetic field lines are obviously not closed. The opened field lines in the lobe are assumed to be reconnected in the far tail (presumably at $X > 80R_E$) under the compression of the solar wind. The intense electric fields related to reconnection are mapped into the ionosphere to form the electric potential configuration shown in Fig. 4. Furthermore the electric fields drive the westward electrojet in the ionosphere. The DDAPCA is caused by the distant X-line.

In general, the onset of the expansion phase of a substorm may be related to the reconnection of the near-Earth closed field lines in the plasma sheet (Baker et al., 1996). Eventually the reconnection reaches the last closed field lines that form the boundary of the plasma sheet. These field lines are normally connected to an inactive, distant X-line located beyond $100R_E$ down the tail (Vasyliunas, 1983). The second stage of the expansion begins when reconnection reaches open field lines in the lobe (Vasyliunas, 1983; Mcpherron, 2005).

Auroral signatures have been observed for highlatitude lobe reconnection during solar wind conditions with high pressure (Frey et al., 2002; Østgaard et al., 2005). Searches for such signatures in connection with tail reconnection have also been made (Ieda et al., 2001; Nakamura et al., 2001).

Kan and Burke (1985) also suggested the polar cap arcs are associated with the distant X-line. If flux is added at the same rate on the dayside as it is removed on the nightside, the open-close field line boundary (OCB) remains stationary. When an active NEXL rapidly reconnects lobe flux during an intense substorm, the nightside OCB expands poleward in the midnight region while open flux is quickly removed from the polar cap (Ober et al., 2001). Thus, the polar cap area shrinks.

The equatorward arc is related to the near-Earth X-line (Nakamura et al., 2001; Wang et al., 2010). Both X-lines along a distant tail (on average near $X_{GSM} = -130R_E$ (Nishida et al., 1996) and at much nearer Earth (20–40R_E) can operate simultaneously (Maynard et al., 1997; Lu et al., 2010).

Another interesting phenomenon is that the DDAPCA turned anticlockwise since 1731 UT and form a tilt angle of 45° with dawn–dusk direction at 1742 UT. It may be associated with the IMF *By* change from positive to negative values, which in turn caused a shift of the neutral line in the far tail. Penetration of IMF *By* into the central plasma sheet can possibly be caused either by magnetic reconnection or diffusion during the growth phase when the near-Earth plasma sheet becomes very thin. Both mechanisms lead to a change of the magnetic topology. This penetration necessarily implies an inter-hemispherical current, and the IMF orientation affects the location of the nightside aurora (Stenbaek-Nielsen and Otto, 1997).

Acknowledgements

We especially thank S.B. Mende and Harald Frey for the use of IMAGE FUV WIC data. The AE data are provided by the World Data Center for Geomagnetism at Kyoto University. Portion of this research were performed at the Jet Propulsion Laboratory, California Institute of Technology, under contract with NASA. This work was supported by NSFC Grants (40890163, 41031066) and Ocean Public Welfare Scientific Research Project, State Oceanic Administration People's Republic of China (No. 201005017). This work was partially supported by RFBR grant nos. 09-05-98546, 11-05-00908 and by SB RAS project no. 69.

References

Akasofu, S.-I., Lui, A.T.Y., Meng, C.-I., 2010. Importance of auroral features in the search for substorm onset processes. J. Geophys. Res. 115, A08218. doi:10.1029/2009JA014960.

Baker, D.N., Pulkkinen, T.I., Angelopulos, V., Baumjohann, W., McPherron, R.L., 1996. Neutral line model of substorms: past results and present view. J. Geophys. Res. 101 (A6), 12875–13010.

Du, A.M., Tsurutani, B.T., Sun, W., 2008. Anomalous geomagnetic storm of 21–22 January 2005: a storm main phase during northward IMFs. J. Geophys. Res. 113, A10214. doi:10.1029/2008JA013284.

Echer, E., Gonzalez, W.D., Tsurutani, B.T., Gonzalez, A.L.C., 2008. Interplanetary conditions causing intense geomagnetic storms (Dst ≤ -100 nT) during solar cycle 23 (1996–2006). J. Geophys. Res. doi:10.1029/2007JA012744.

Echer, E., Tsurutani, B.T., Guarnierid, F.L., Kozyra, J.U., 2011. Interplanetary fast forward shocks and their geomagnetic effects: CAWSES events. Journal of Atmospheric and Solar-Terrestrial Physics 73 (11–12), 1330–1338. doi:10.1016/j.jastp.2010.09.020.

Elphinstone, R.D., Murphree, J.S., Heam, D.J., Sandahl, I., Cogger, L.L., Newell, P.T., Klumpar, D.M., Ohtani, S., Potemra, T.A., Sauvaud, J.A., Mursula, K, Wright, A., Shapshak, M., 1995. The double oval UV auroral distribution 1. implications for the mapping of auroral arcs. J. Geophys. Res. 100 (A7), 12,075–12,092.

Feldstein, Y.I., Starkov, G.V., 1967. Dynamics of auroral belt and polar geomagnetic disturbances. Planet. Space Sci. 15, 209–230.

Frey, H.U., et al., 2002. Proton aurora in the cusp. J. Geophys. Res. 107 (A7), 1091. doi:10.1029/2001JA900161.

Ieda, A., Fairfield, D.H., Mukai, T., Saito, Y., Kokubun, S., Liou, K., Meng, C.-I., Parks, G.K., Brittnacher, M.J., 2001. Plasmoid ejection and auroral brightenings. J. Geophys. Res. 106, 3845–3858.

Kamide, Y., Richmond, A.D., Matsushita, S., 1981. Estimation of ionospheric electric fields, ionospheric currents, and field-aligned currents from ground magnetic records. J. Geophys. Res. 86, 801.

Kan, J.R., Burke, W.J., 1985. A theoretical model of polar cap auroral arcs. J. Geophys. Res. 90, 4171.

Knipp, D.J., 1993. Ionospheric convection response to slow, strong variations in a northward interplanetary magnetic field: a case study for January 14, 1988. J. Geophys. Res. 98 (19), 273.

Kornilova, T.A., Kornilov, I.A., 2006. Auroral intensification structure and dynamics in the double oval: substorm of December 26, 2000. Geomagn. Aeron. 46 (4), 450–456. doi:10.1134/S0016793206040062.

Lassen, K., Danielsen, C., 1989. Distribution of auroral arcs during quiet geomagnetic conditions. J. Geophys. Res. 94 (A3), 2587–2594. doi:10.1029/JA094iA03p02587.

Lu, Q., Huang, C., Xie, J.L., Wang, R.S., Wu, M.Y., Vaivads, A., Wang, S., 2010. Features of separatrix regions in magnetic reconnection: comparison of 2D particle-in-cell simulations and cluster observations. J. Geophys. Res. 115, A11208. doi:10.1029/2010JA015713.

Maynard, N.C., et al., 1997. Geotail measurements compared with the motions of high-latitude auroral boundaries during two substorms. J. Geophys. Res. 102, 9553.
Mcpherron, R.L., 2005. Magnetic pulsations: their sources and relation to solar wind and geomagnetic activity. Surv. Geophys. 26, 545–592.
Mende, S.B., Heetderks, H., Frey, H.U., 2000a. Far ultraviolet imaging from the IMAGE spacecraft 1. system design. Space Sci. Rev. 91, 243–270.
Mende, S.B., Heetderks, H., Frey, H.U., 2000b. Far ultraviolet imaging from the IMAGE spacecraft. 2. Wideband FUV imaging. Space Sci. Rev. 91, 271–285.
Nakamura, R., Baumjohann, W., Brittnacher, M., Sergeev, V.A., Kubyshkina, M., Mukai, T., Liou, K., 2001. Flow bursts and auroral activations: onset timing and foot point location. J. Geophys. Res. 106, 10,777–10,790.
Newell, Patrick T., Liou, Kan, Meng, Ching-I., Mitchell, J., Brittnacher, Parks, George, 1999. Dynamics of double-theta aurora: polar UVI study of January 10-11, 1997. J. Geophys. Res. 104 (A1), 95–104.
Nishida, A., Mukai, T., Yamamoto, T., Saito, Y., Kokubun, S., 1996. Magnetotail convection in geomagnetically active times, 1, Distance to the neutral lines. J. Geomagn. Geoelectr. 48, 489.
Nykyri, K., Otto, A., 2001. Plasma transport at the magnetospheric boundary due to reconnection in Kelvin–Helmholz vortices. Geophy. Res. Lett. 28 (18), 3565–3568.
Ober, D.M., Maynard, N.C., Burke, W.J., Peterson, W.K., Sigwarth, J.B., Frank, L.A., Scudder, J.D., Hughes, W.J., Russell, C.T., 2001. Electrodynamics of the poleward auroral border observed by Polar during a substorm on April 22, 1998. J. Geophys. Res. 106, 5927.
Otto, A., Fairfield, D.H., 2000. Kelvin–Helmholz instability at the magnetotail boundary: MHD simulation and comparison with Geotail observations. J. Geophys. Res. 105 (A9), 21175–21190.
Østgaard, N., Mende, S.B., Frey, H.U., Sigwarth, J.B., 2005. Simultaneous imaging of the reconnection spot in the conjugate hemispheres during northward IMF. Geophys. Res. Lett. 32 (21), L21104. doi:10.1029/2005GL024491.
Stenbaek-Nielsen, H.C., Otto, A., 1997. Conjugate auroras and the interplanetary magnetic field. J. Geophys. Res. 102 (A2), 2223–2232.
Sun, W., Zhou, X.-Y., Du, A., 2008. Quantitative separation of the directly-driven and unloading components of the ionospheric electric field. Geophys. Res. Lett. 35, L13104. doi:10.1029/2008GL033931.
Tsurutani, B.T., et al., 1998. The January 10, 1997 auroral hot spot, horseshoe aurora and first substorm: a CME loop? Geophys. Res. Lett. 25 (15), 3047–3050. doi:10.1029/98GL01304.
Tsurutani, B.T., Zhou, X.-Y., Vasyliunas, V.M., Haerendel, G., Arballo, J.K., Lakhina, G.S., 2001a. Interplanetary shocks, magnetopause boundary layers and dayside auroras: the importance of a very small magnetospheric region. Surveys in Geophys. 22, 101.
Tsurutani, B.T., et al., 2001b. Auroral zone dayside precipitation during magnetic storm initial phases,. J. Atmos. Terr. Phys. 63, 513–522.
Vasyliunas, V.M., 1983. Large-scale Morphology of the Magnetosphere. In: Carovillano, R.L.A.F., Forbs, J.M. (Eds.), Solar-Terrestrial Physics: Principles and Theoretical Foundations. D. Reidel Publishing Company, Dordrecht, pp. 243–254.
Wang, R., Lu, Q., Huang, C., Wang, S., 2010. Multispacecraft observation of electron pitch angle distributions in magnetotail reconnection. J. Geophys. Res. 115, A01209. doi:10.1029/2009JA014553.
Zhang, J., et al., 2007. Solar and interplanetary sources of major geomagnetic storms ($Dst \leq -100$ nT) during 1996–2005. J. Geophys. Res 112, A10102. doi:10.1029/2007JA0123 21.
Zhou, X., Tsurutani, B.T., 2001. Interplanetary shock triggering of nightside gomagnetic activity: substorms, pseudobreakups, and quiescent events. J. Geophys. Res. 106 (A9), 18957–18967.
Zhou, X.-Y., Tsurutani, B.T., Mende, S.B., Frey, H.U., Watermann, J.F., Sibeck, D.G., Arballo, J.K., 2001. Dawn/dusk aurora and propagating convection disturbance: ionospheric effects of high solar wind ram pressures, LLBL New Orleans Chapman Conference, 8/20/2001, New Orleans, LA, USA.
Zhou, X.-Y., Strangeway, R.J., Anderson, P.C., Sibeck, D.G., Tsurutani, B., Haerendel, G., Frey, H.U., Arballo, J.K., 2003. Shock aurora: FAST and DMSP observations. J. Geophys. Res. 108, 8019 (17pp). doi:10.1029/2002JA009701.